Published online in advance by J-STAGE

J Prosthodont Res. 2026; **(**): ****–****

OPEN ACCESS JPR Prosthodontic Research

Journal of Prosthodontic Research

Original article

# Stress distribution of inlay, onlay, and overlay restorations across materials: A finite element study

Sedef Kurt [a,*], Zeynep Yeşil [b]

[a] Department of Prosthodontics, Faculty of Dentistry, Recep Tayyip Erdoğan University, Rize, Türkiye, [b] Department of Prosthodontics, Faculty of Dentistry, Atatürk University, Erzurum, Türkiye

**Abstract**

**Purpose:** We evaluated the stress distribution patterns in inlay, onlay, and overlay restorations fabricated from different CAD-CAM materials, including current 3D-printed resins and 3D-printed zirconia, under 300 N vertical loading using finite element analysis (FEA).

**Methods:** A 3D solid model of a mandibular first molar was generated based on standard anatomical dimensions. Fifteen finite element models were constructed by combining three preparation designs with five restorative materials. A static vertical load of 300 N was applied and distributed across the multipoint occlusal contacts to simulate physiological masticatory forces. The stress distribution was analyzed using the von Mises and Maximum Principal Stress criteria to evaluate both the restoration and the surrounding dental tissues.

**Results:** Restoration design and material stiffness significantly influenced stress distribution. Among the designs, the overlay preparations exhibited the most favorable biomechanical behavior, showing lower stress transmission to the tooth structure than inlay and onlay designs. Materials with a high elastic modulus (205.000 MPa LithaCon 3Y-210) demonstrated a stress-shielding effect, absorbing higher internal stress while protecting the underlying dentin. Conversely, low-modulus materials (4.030 MPa VarseoSmile Crown Plus) exhibited lower internal stress, but transferred higher stress loads to the tooth-restoration interface and dentin.

**Conclusions:** The use of overlay designs combined with high-elastic modulus materials offers a biomechanically superior configuration for reinforcing compromised posterior teeth because this combination minimizes stress transmission to the remaining tooth structure. Although low-modulus materials reduce internal restoration stress, they require careful consideration because of the increased stress transfer to the dentin.

**Keywords:** Inlay, Onlay, Overlay, Finite Element Stress Analysis, Zirconia

Received 30 September 2025, Accepted 24 February 2026, Available online 18 March 2026

## 1. Introduction

Crowns are classified as temporary or permanent according to their intended use, and as full or partial according to the extent of coverage. Full crowns cover the entire coronal portion of the tooth, whereas partial crowns cover only one portion. Restorations that partially cover the natural crown include 3/4, 4/5, and 7/8 crowns, ceramic inlays, ceramic onlays, ceramic overlays, and ceramic veneers[1].

The paradigm shift toward minimally invasive dentistry has favored the use of defect-oriented partial restorations, such as inlays, onlays, and overlays, over traditional full-coverage crowns to preserve healthy tooth structure[2]. Although these restorations offer superior esthetics and anatomical preservation, their long-term clinical success relies heavily on the complex biomechanical interaction between the preparation design (geometry) and the restorative material[3]. Specifically, preservation or reduction of weakened cusps plays a critical role in mitigating the risk of postoperative fractures under occlusal loading[4].

The occlusal thickness should be 1.5–2.5 mm for ceramic inlay/onlay restorations; maintaining uniform material thickness across regions increases clinical success[5]. The occlusal width (buccolingual dimension) of the cavity should be at least 2 mm[6]. An occlusal thickness of 2.0 mm is considered ideal for ceramic inlays and onlays with functional cusps. Occlusal bevels should be avoided as they

***WHAT IS ALREADY KNOWN ABOUT THE TOPIC?***

» *Restoration design and material stiffness influence biomechanics; however, comparative data on modern 3D-printed zirconia and resins across different designs are limited.*

***WHAT THIS STUDY ADDS?***

» *High-modulus 3D-printed zirconia overlays exhibit a "stress-shielding" effect, protecting the tooth structure better than flexible resins, which transfer higher loads to the dentin.*

**DOI:** https://doi.org/10.2186/jpr.JPR_D_25_00304

***Corresponding author:** Sedef Kurt, İslampaşa, Menderes Boulevard No:612, 53020 Rize Merkez, Rize, Türkiye.

**E-mail address:** sedef.kurt@erdogan.edu.tr

create thin porcelain margins prone to fracture under occlusal stress; instead, a butt-joint preparation is recommended to ensure adequate material thickness[7]. Furthermore, weakened cusps (<2 mm in thickness) must be included in the preparation (cuspal coverage) to enhance fracture resistance[8].

Partial indirect ceramic restorations are produced using subtractive methods (CAD-CAM milling) and are increasingly produced using additive methods (3D printing)[9]. Current CAD-CAM technologies offer a diverse spectrum of materials with varying elastic moduli to optimize stress distribution. We selected five distinct material classes to evaluate the impact of material stiffness and manufacturing techniques.

**Lithium disilicate (IPS e.max CAD):** Selected as the clinical "gold standard" and control group due to its documented high survival rates and mechanical reliability[10].

**Lithography-based 3D-printed 3 mol% yttria-stabilized zirconia (LithaCon 3Y-210):** Included to represent high-strength glass ceramics that combine esthetics with improved mechanical properties owing to the dissolved zirconia content[11].

**Resin-matrix ceramics (VITA Enamic & Lava Ultimate):** These were selected for their lower elastic moduli, designed to mimic natural dentin, and provide a stress-dampening effect[12].

**3D-printed permanent resin (VarseoSmile Crown Plus):** This study investigated the biomechanical behavior of an emerging additive manufacturing technology compared with established subtractive (milled) methods[13].

Finite element analysis (FEA) is a powerful noninvasive tool for simulating complex biomechanical scenarios and predicting internal stress concentrations that are impossible to measure *in vivo*[14]. Although numerous FEA studies have evaluated the behavior of traditional CAD-CAM materials, data on the comparative performance of recently introduced 3D-printed permanent resins (such as VarseoSmile Crown Plus) and novel 3D-printed zirconia (such as LithaCon 3Y-210) are scarce. Furthermore, the current literature lacks a comprehensive consensus on how these specific novel materials interact with different preparation designs (inlay, onlay, and overlay) under identical loading conditions. Most existing studies have focused on either material properties or cavity design in isolation, leaving a gap in the understanding of the combined effects of material stiffness and restoration geometry on stress distribution.

Despite the clinical availability of these materials, limited data exist on the stress distribution patterns of novel 3D-printed resins and zirconia in different cavity designs. Therefore, we evaluated the stress distribution patterns in inlay, onlay, and overlay restorations fabricated from diverse CAD-CAM materials under 300 N vertical loading using FEA.

## 2.Materials and Methods

### *2.1. Study design*

The geometric model of the mandibular first molar was generated based on standard anatomical dimensions from Wheeler's Dental Anatomy to ensure geometric consistency and represent an ideal tooth morphology free from individual variations such as attrition. Conversely, the supporting mandibular bone structure (cortical and cancellous bone) was derived from the CBCT data of a healthy patient to simulate realistic support conditions. A mandibular bone model was generated from a computed tomography (CT) scan of an edentulous adult. The dataset was reconstructed with a 0.1 mm slice thickness and imported into a 3D Slicer in DICOM format. Appropriate Hounsfield-unit (HU) thresholds in 3D Slicer were used to segment the DICOM data and obtain a 3D model, which was subsequently exported in the STL format. The STL models were imported into Blender (Blender Foundation; Amsterdam, Netherlands), and a uniform 2 mm offset was applied to the mandibular model to define a 2 mm-thick cortical shell. The trabecular compartment was derived by referring to the inner surface of the cortical shell. The standardized tooth model was aligned and embedded in the alveolar bone socket, and congruent interfaces were established using Boolean subtraction. Minor surface-smoothing algorithms were applied to the CBCT-derived mandibular bone model to eliminate segmentation noise and artifacts and ensure mesh continuity.

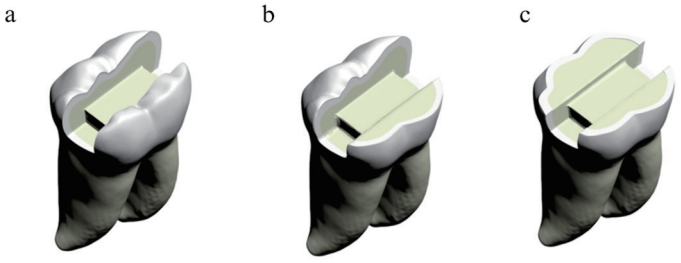


**Fig. 1.** Cavity designs used in the study: (a) inlay; (b) onlay; (c) overlay. Preparations illustrate marginal extents and cusp coverage for each design.

Inlay, onlay, and overlay designs were developed to restore three different magnitudes of material losses in the first molar. Five distinct restorative materials were modeled for each design. In each model, a MOD retention cavity was prepared with the internal walls diverging occlusally by 6 degrees and a depth of 2 mm. Restoration lengths were set to match the 7.5 mm crown height in accordance with the Wheeler atlas data. Gingival steps with a width of 1 mm and positioned 1.5 mm coronal to the cementoenamel level were prepared. The buccolingual length of the inlay cavity was modeled as one-third of the buccolingual length of the tooth, which is consistent with the literature (**Fig. 1a**). A modified inlay form was used for the onlay configuration, with a 2 mm occlusal reduction at the lingual cusps (**Fig. 1b**). A modified inlay form was used for the overlay configuration, with a 2 mm occlusal reduction at both the lingual and buccal cusps (**Fig. 1c**).

### *2.2. Fabrication of fixed partial restorations*

Fixed partial restorations were fabricated using the restorative materials listed in **Table 1.**

### *2.3. Obtaining mathematical models*

Finite-element (mathematical) models were obtained by discretizing the geometric models into small, simple elements (meshes). After modeling in Blender, the models were discretized and prepared for analysis using ALTAIR HyperMesh. Surface-meshes were generated using triangular elements (tria) with a high-resolution target size of 0.10–0.25 mm. Subsequently, volumetric meshes were con-

**Table 1.** Fixed partial restorative materials used in the study

| Commercial Name | Material Type | Manufacturer |
|---|---|---|
| IPS Emax CAD | Lithium disilicate reinforced Glass ceramic blocks | Ivoclar Vivadent; Schann, Liechtenstein |
| Lava Ultimate | Nanoceramic ceramic blocks | 3M Espe; Seefeld, Germany |
| Vita Enamic | Hybrid ceramic blocks | Vita, Bad Sackingen Germany |
| Lithacon 3Y 210 | Light-curing resin matrix 3-mol% yttrium-stabilized zirconia ceramic powder and additives | Lithoz; Wien, Austria |
| VarseoSmile Crown Plus | 3D printed hybrid resin Composite | Bego; Bremen, Germany |

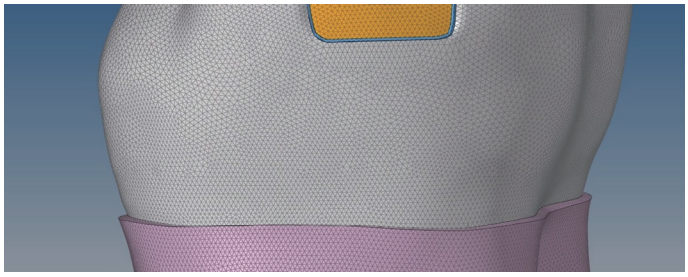

**Fig. 2.** Generation of the numerical model. The 3D geometry was modeled in Blender, meshed in ALTAIR HyperMesh, and prepared for the ALTAIR OptiStruct solver.

structed using regular tetrahedral solid elements. Next, the finalized models were transferred from the ALTAIR HyperMesh to the ALTAIR OptiStruct solver for analysis (**Fig. 2**). A mesh convergence test was conducted to verify the reliability of the finite element model, and the resulting graph is presented in **Figure 3**.

### *2.4. Material definitions*

The linear properties of the materials were used in the analyses, given their elastic moduli and Poisson's ratios. The material properties of the analyzed model were defined numerically in **Table 2.**

### *2.5. Loading scenarios and boundary conditions*

A vertical load of 300 N was applied on the central fossa to simulate the primary closure phase of the masticatory cycle (maximum intercuspation). Because the oral environment involves complex multidirectional forces, a vertical loading vector was selected to standardize the assessment of the stress transmission properties of different material classes without confounding variables of lateral vector components.

A vertical load of 300 N was applied at three locations in inlay and onlay models: central fossa, mesial marginal ridge, and distal marginal ridge (**Fig. 4a, b**). A total vertical load of 300 N was applied at five locations in the overlay model: central fossa, distobuccal and mesiobuccal cusp tips, and mesial and distal marginal ridges (**Fig. 4c**). Loads were distributed to neighboring nodes to avoid stress singularities at contact regions. The boundary conditions were imposed by fully constraining all degrees of freedom at the nodes in the anterior, posterior, and inferior regions of the bone, thereby preventing motion along all three axes. In total, 15 linear static analyses were performed across the three model types under loading and boundary conditions.

### *2.6. Quantitative model information*

Information on element and node numbers for different analysis models is provided in **Table 3**.

### *2.7. Combining systems and interconnectedness of parts*

The luting cement layer was not geometrically modeled with a specific thickness to optimize the mesh quality and computational efficiency. Instead, a perfect bonding condition was assumed between the restoration intaglio surface and the prepared cavity walls to simulate the clinical adhesive cementation procedure. A freeze-type contact was assigned across all contact regions, assuming perfectly correlated motion between the parts (i.e., no relative displacement).

## 3. Results

Statistical testing was not conducted because the outputs were deterministic results of mathematical calculations without variance. The stress distributions and concentration zones were assessed by examining von Mises stress (VMS) maps. Red denotes regions of maximum stress in the images, whereas colors shifting toward blue indicate decreasing stress magnitudes. Red corresponds to the highest tensile stress in the maps of maximum principal stress, which is reported as a positive value. All stress values are expressed in $N/mm^2$ (MPa). The findings are supported by tables and figures. Cross-sectional views were interpreted with reference to nodal stress magnitudes and distributions.

Across the inlay, onlay, and overlay configurations, von Mises stress (VMS) concentrations were consistently localized at the occlusal loading sites, retention cavities, and step regions. Quantitative analysis revealed that LithaCon 3Y-210 exhibited the highest peak VMS value, reaching approximately 1225.876 MPa, corresponding to the red zones on the colorimetric scale. The VMS magnitude followed a descending order, consistent with the elastic moduli of the materials: LithaCon 3Y-210 > IPS e.max CAD (1221.283 MPa) > VITA Enamic (1186.568 MPa) > Lava Ultimate (943.972 MPa) > VarseoSmile Crown Plus (939.994 MPa). Regarding cavity design, onlay restorations yielded higher overall VMS concentrations (peaking at 1225.876 MPa) than other configurations (**Fig. 5**).

An evaluation of the stress distributions within the enamel revealed that the stress concentrations were topographically similar across all groups and were primarily localized at the cervical margins and proximal contact areas. However, the surface area of the enamel subjected to stress was notably larger in the models utilizing VarseoSmile Crown Plus. Stress propagation extended broadly into the cervical region in these models, represented by extensive red zones corresponding to the 39.843–49.478 MPa range. Quantitatively, the onlay restorations exhibited the highest peak von Mises

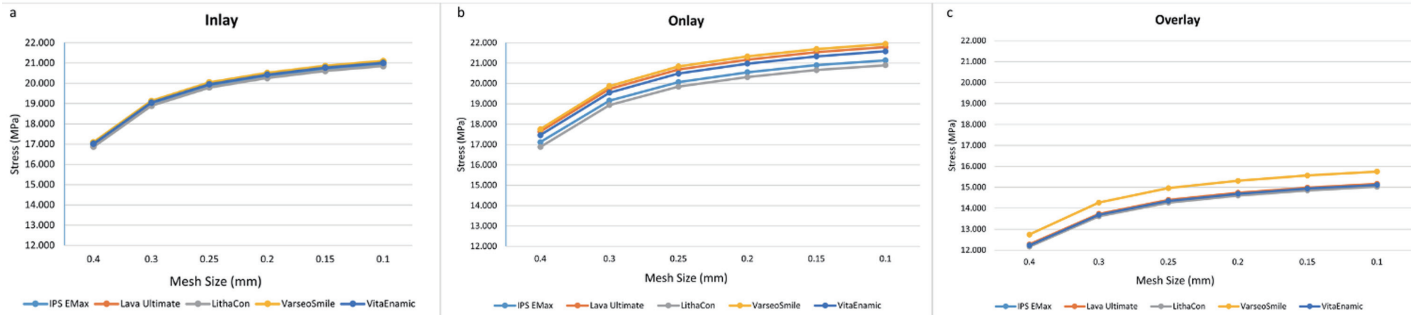


**Fig. 3.** Mesh convergence analysis for the three restoration designs: (a) inlay, (b) onlay, and (c) overlay.

**Table 2.** Material descriptions

| Material | Elastic modulus | Poisson's ratio | References |
|---|---|---|---|
| Cortical bone | 13700 | 0.3 | [15] |
| Trabecular bone | 1370 | 0.3 | [15] |
| Dentin | 18600 | 0.31 | [15] |
| Enamel | 84100 | 0.33 | [15] |
| Periodontal ligament | 70 | 0.45 | [15] |
| IPS Emax CAD | 102700 | 0.22 | [16] |
| Lava Ultimate | 12700 | 0.45 | [17] |
| Vita Enamic | 34700 | 0.28 | [18] |
| LithaCon 3y210 | 205000 | 0.3 | [19] |
| VarseoSmile Crown Plus | 4030 | 0.3 | [20] |
| Panavia F2.0 resin cement | 12000 | 0.33 | [21] |

**Table 3.** Model information

| | Total number of nodes | Total number of elements |
|---|---|---|
| **Inlay** | 521,666 | 2,049,069 |
| **Onlay** | 519,388 | 2,038,700 |
| **Overlay** | 523,634 | 2,054,613 |

stress values within the enamel structure, reaching approximately 50.247 MPa (indicated by red focal points on the scale), compared to the inlay and overlay groups (**Fig. 6**).

Regarding the tensile stress distribution, models restored with VarseoSmile Crown Plus exhibited a broader stress propagation pattern within the enamel than other groups. This was visually characterized by extensive red zones, corresponding to an intermediate tensile stress range of 36.000–78.000 MPa. In terms of peak intensity, the onlay restorations recorded the highest Maximum Principal Stress (MPS) values, indicated by red areas, reaching approximately 78.404 MPa. Conversely, the overlay designs demonstrated the most favorable biomechanical behavior. The enamel regions subjected to high tensile stress were significantly reduced, predominantly displaying blue (low-stress) patterns ranging from 12.188 MPa (**Fig. 7**).

In the dentin structure, while the topographic localization of stress was consistent across groups (concentrated at the pulpal floor and cavity walls), the magnitude of the transmitted stress varied significantly based on the material stiffness. The models restored with the low-modulus VarseoSmile Crown Plus exhibited the highest stress transmission to dentin. Stress accumulation extended to the cavity step and internal angles in these models, represented by red zones, reaching peak von Mises values of approximately 21.940 MPa. Conversely, the high-modulus LithaCon 3Y-210 demonstrated a protective effect, resulting in the lowest stress values in the dentin (15.021 MPa), as indicated by blue areas. Consequently, the descending order of stress magnitude in dentin was VarseoSmile Crown Plus > Lava Ultimate > VITA Enamic > IPS e.max CAD > LithaCon 3Y-210 (**Fig. 8**).

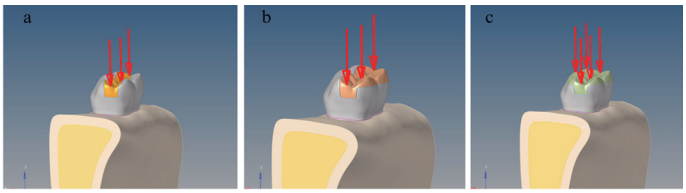


**Fig. 4.** Loading and constraint scheme. (a, b) Application of a 300 N vertical load at multiple occlusal contact points for inlay and onlay models; (c) identical loading for the overlay model. Root constraints are shown for reference.

Maximum principal stress (MPS) analysis of dentin revealed tensile stress concentrations predominantly at the internal line angles and cavity steps in all groups. However, the intensity of these tensile forces is strongly influenced by the restorative material. The VarseoSmile Crown Plus group (specifically the onlay design) transferred the highest tensile loads to dentin. These critical areas are depicted as red zones on the scale, reaching a maximum value of 12.109 MPa. Conversely, LithaCon 3Y-210 exhibited the lowest dentinal MPS value of 2.236 MPa (represented by blue regions), indicating superior protection of the tooth structure against tensile failure compared with the other material groups (**Fig. 9**).

To evaluate the risk of biomechanical failure, the peak von Mises stress values observed in the tooth structure were compared with the reported ultimate tensile strengths (UTS) of dental tissues. The UTS of enamel is generally reported to be in the range of 80–100 MPa, whereas that of dentin exhibits a UTS ranging from 40 to 105 MPa, depending on the orientation and location of the tubules[22]. In the present study, the stress concentrations in the tooth structure remained below these critical thresholds for most restoration designs, suggesting a low risk of immediate fracture under static loading. However, the higher stress transfer observed in low-modulus materials suggests that fatigue failure over time remains a concern[22].

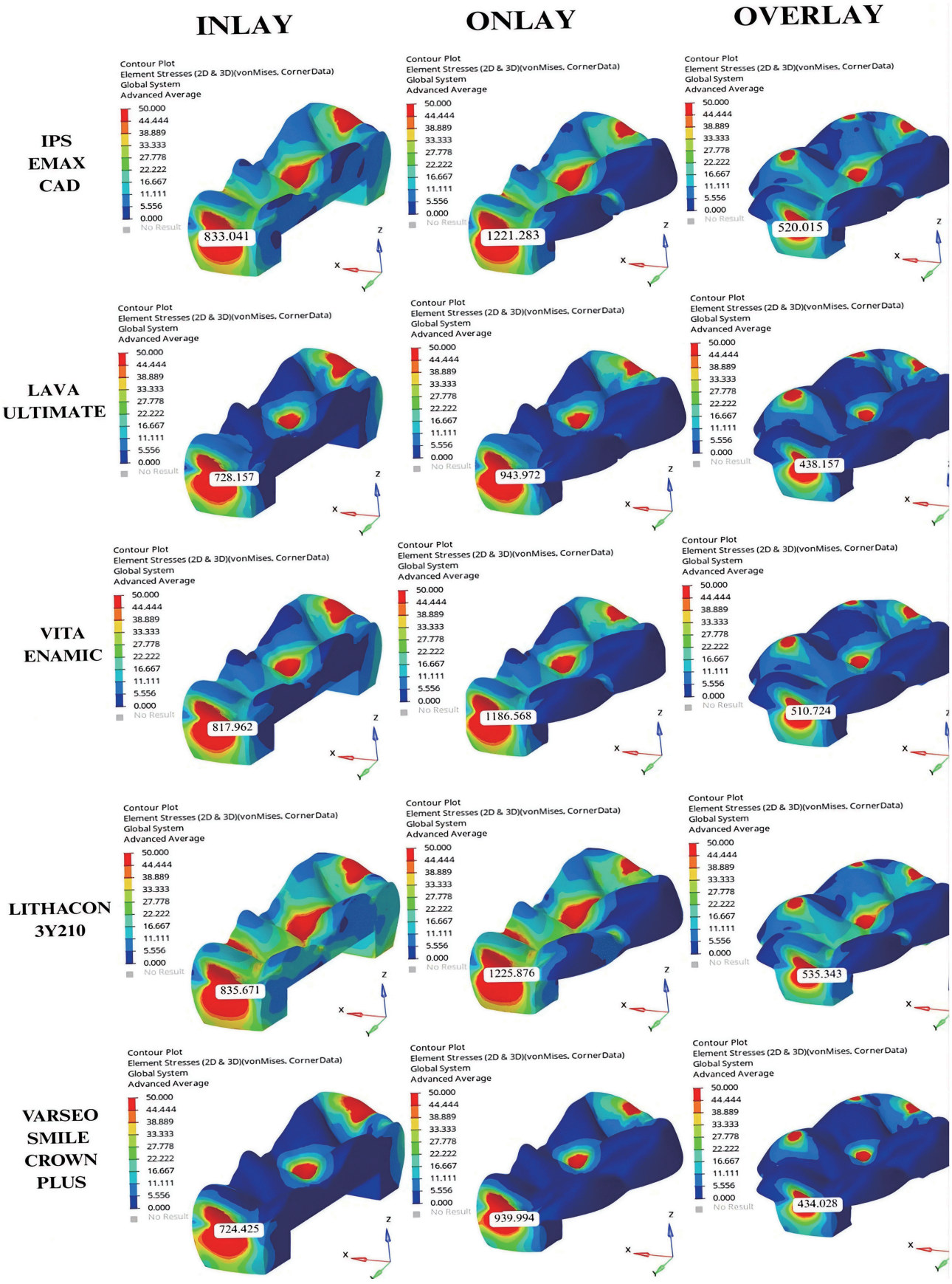


**Fig. 5.** VMS distributions within the restoration for inlay, onlay, and overlay designs under 300 N loading. A common color scale is used across panels (units: MPa). VMS: von Mises stress; MPa: megapascal.

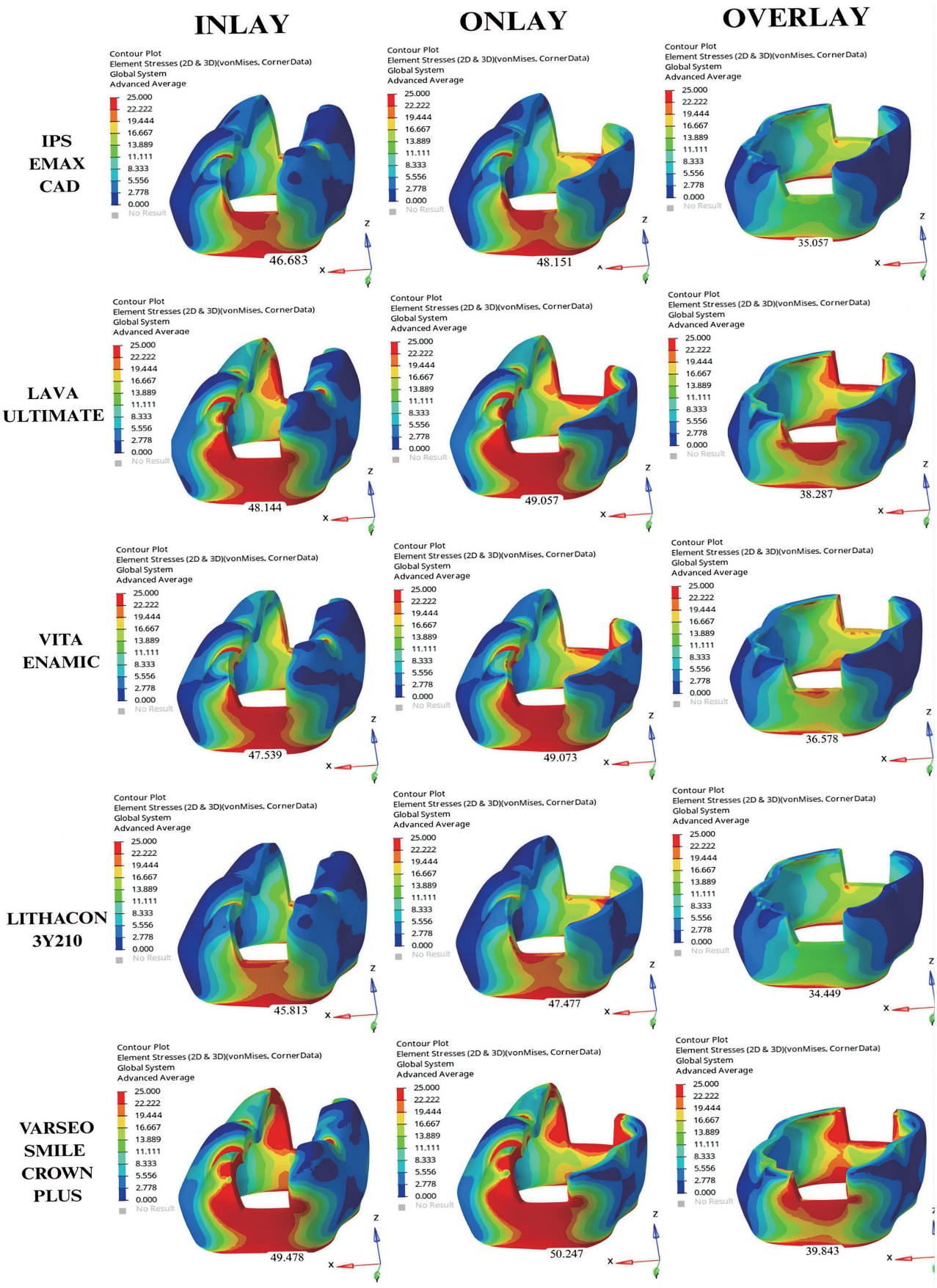


**Fig. 6.** VMS distributions in enamel under 300 N loading for the three cavity designs (units: MPa). VMS: von Mises stress; MPa: megapascal.

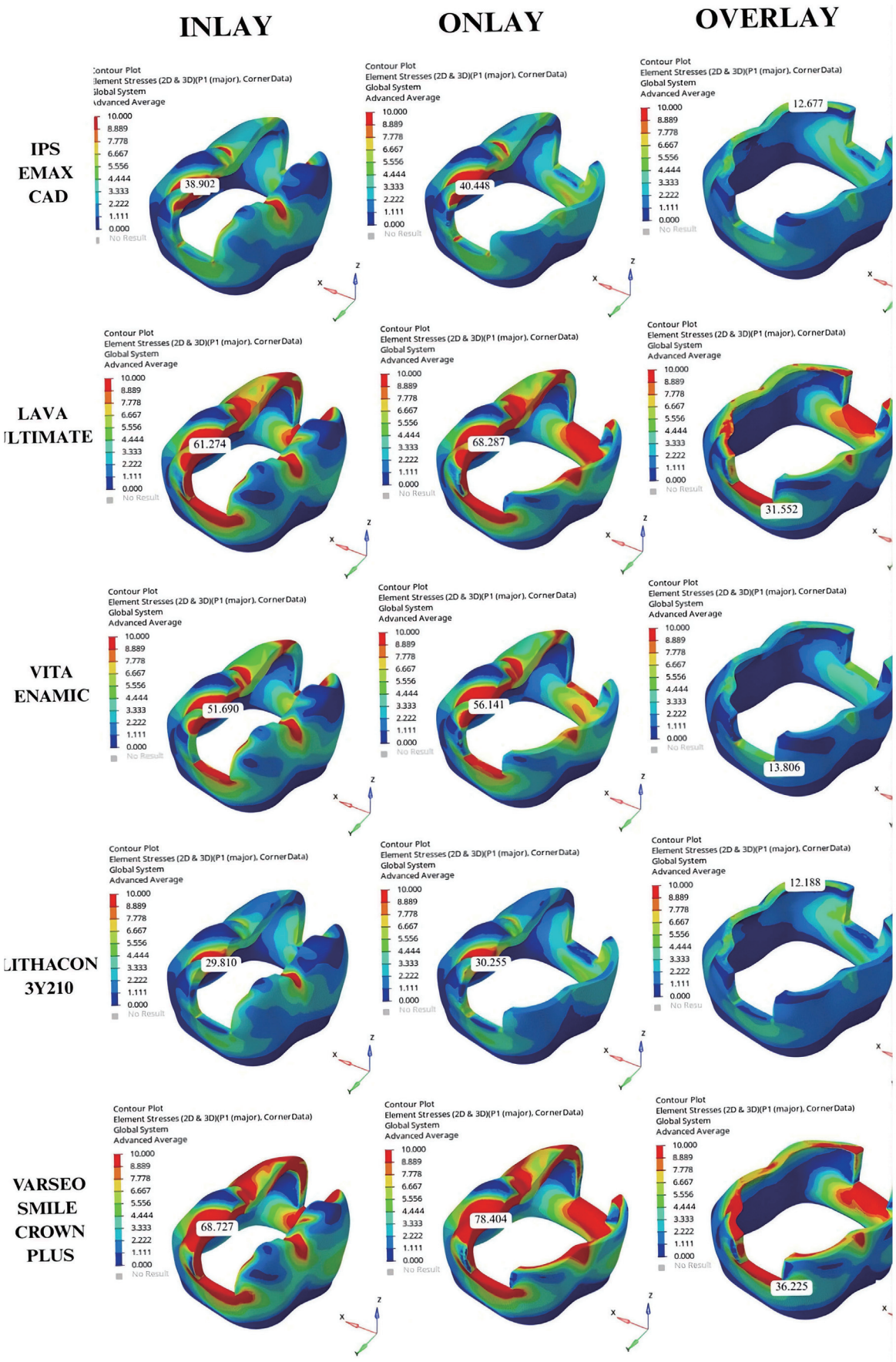


**Fig. 7.** Maximum principal (tensile) stress fields in enamel under 300 N loading for the three cavity designs (units: MPa). MPa: megapascal.

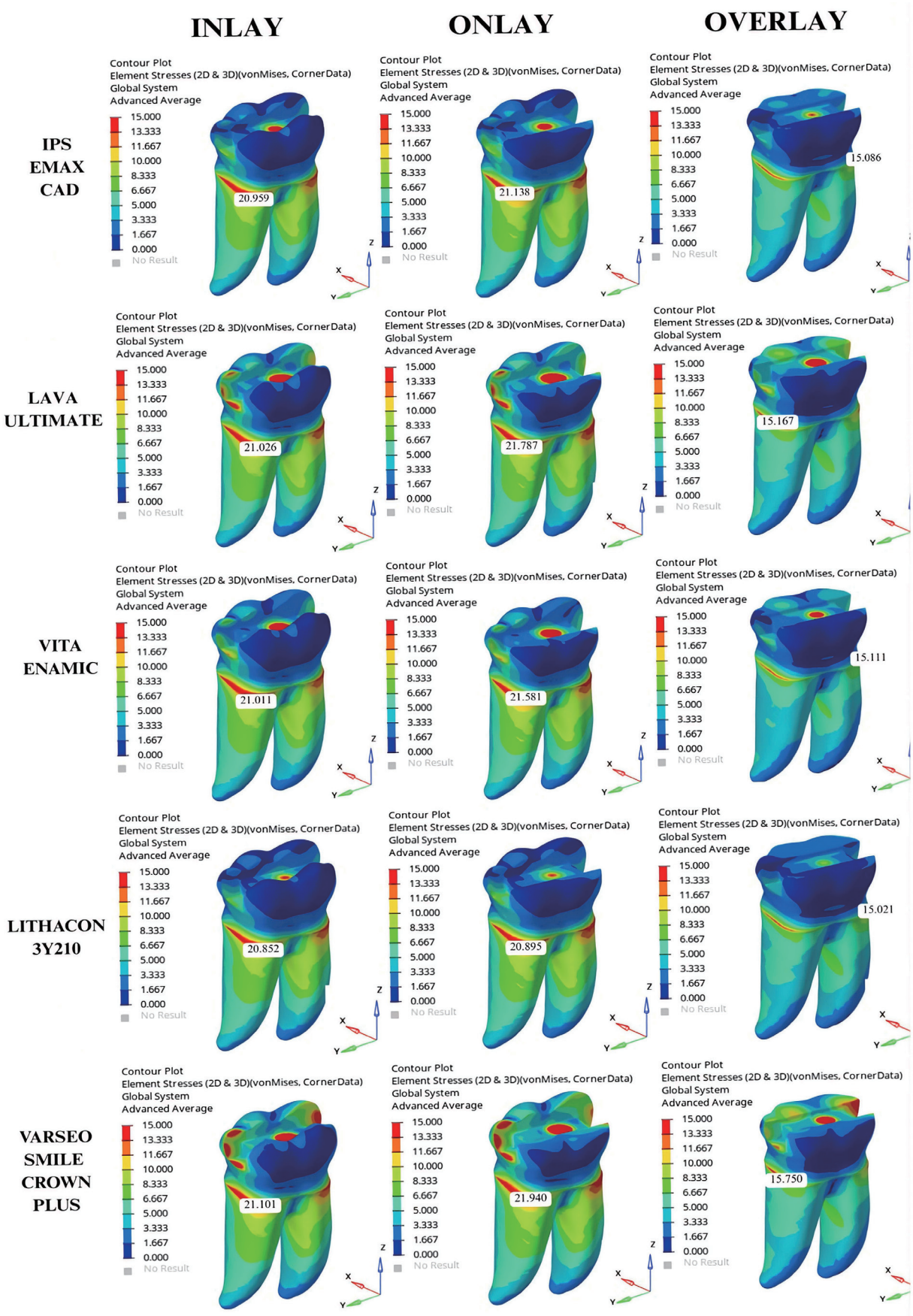


**Fig. 8.** VMS distributions in dentin under 300 N loading for the three cavity designs (units: MPa). VMS: von Mises stress; MPa: megapascal.

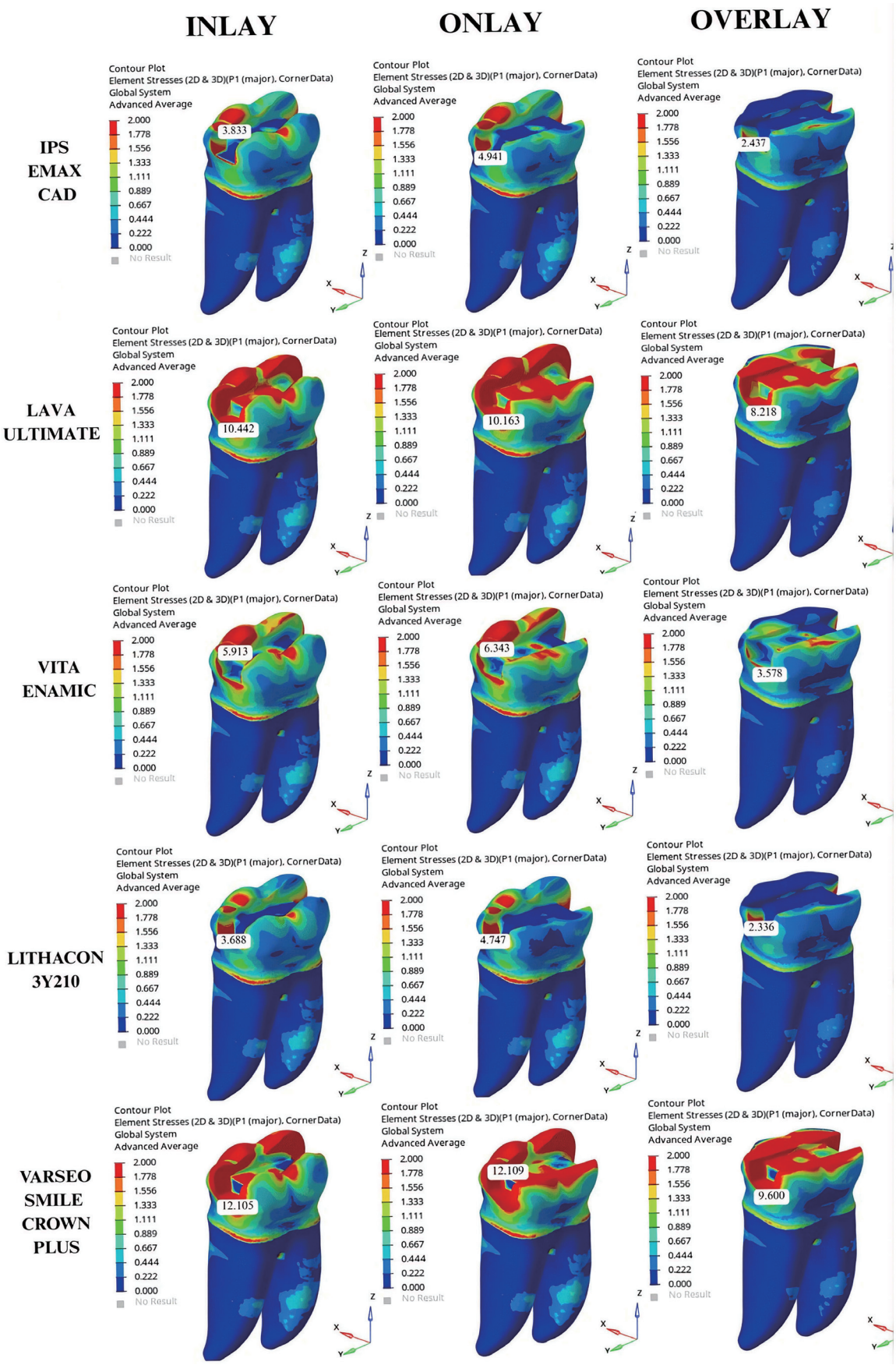


**Fig. 9.** Maximum principal (tensile) stress fields in dentin under 300 N loading for the three cavity designs (units: MPa). VMS: von Mises stress; MPa: megapascal.

A direct correlation was observed between the elastic modulus of the restorative materials and stress distribution patterns. Materials with higher elastic moduli (e.g., LithaCon 3Y-210) exhibited higher von Mises stress values within the restoration body, thereby shielding the underlying tooth structure. Conversely, lower-modulus materials (e.g., Lava Ultimate and VarseoSmile) displayed lower internal stress concentrations but transferred higher stress loads to the dentin and enamel. In addition, the peak stress values in the tooth structure were evaluated against the reported ultimate tensile strengths of dentin (~40–50 MPa) and enamel (~80–100 MPa) to assess the risk of biomechanical failure. We revised the Results section to include a correlation statement linking the elastic modulus of the material to its stress behavior. We found that stiffer materials absorb more stress (stress shielding), whereas more flexible materials transfer the load to the tooth. Furthermore, we included reference values for the ultimate tensile strength of enamel and dentin to contextualize the tissue risk.

## 4. Discussions

Corsentino *et al.* reported indirect restorations to be suitable for long-term functional and aesthetic success in teeth lacking mesial and distal marginal ridges[23]. The literature suggests no fixed rule for inlay preparation; therefore, it is crucial to follow the manufacturer's instructions for the selected material. The cavity should be shaped to provide sufficient restorative thickness and minimize fracture risk[24]. The central fossa depth should be at least 2 mm for ceramic inlays, whereas it should be at least 1.5 mm for composite inlays[24].

Ho *et al.* stated that modeling the cementum in FEA studies is unnecessary because it is a thin layer whose elastic modulus is considered equivalent to that of dentin. Accordingly, the cementum was considered part of the dentin in the present study, and its thickness was not included in the calculations[25].

Hidaka *et al.*[26] reported that the maximum bite force in the molar region ranged from 600 to 800 N, and Gibbs *et al.*[27] reported that the force during swallowing was approximately 300 N. Yoon *et al.*[28] investigated the effects of different post placements on stress distribution in mandibular first molars under an occlusal force of 300 N using the FEA method. Dartora *et al.*[29] compared the stress distribution of endocrown restorations fabricated from different CAD-CAM materials under 300 N loading in root canal-treated mandibular molars using FEA. Therefore, the posterior restorations must be sufficiently durable to tolerate these forces. Therefore, we applied a multipoint loading of 300 N to simulate the intraoral occlusal environment and create broad contact areas.

Previous finite element studies have indicated that cement layer thicknesses up to 70–100 μm do not significantly alter the global stress distribution patterns within the restoration-tooth complex[30]. The interface between the restoration and the tooth structure was defined using a "bonded" contact condition (freeze contact) in the present analysis. This assumption simulates the ideal clinical scenario of adhesive cementation, where resin cements create a "monoblock" effect, ensuring continuous stress transmission from the restorative material to the underlying dentin without interfacial sliding or separation. We employed this contact type to focus on the stress distribution behavior of restorative materials under optimal bonding conditions rather than evaluating the failure modes of the adhesive interface.

We evaluated both von Mises stress (VMS) and maximum principal stress (MPS) values to provide a comprehensive biomechanical profile. While the MPS is widely accepted as the gold standard for predicting failure in brittle materials (such as ceramics and enamel) by highlighting tensile stress concentration areas prone to crack initiation, the von Mises stress provides an overview of the total stress intensity[31]. Given that resin-based composites and hybrid materials exhibit "quasi-brittle" behavior owing to their polymer matrix, which possesses slight ductility compared to pure ceramics[32], the von Mises stress remains a relevant metric for assessing the distortion energy that could lead to matrix yielding, while also facilitating comparison with the extensive existing literature that predominantly employs this criterion[33]. While advanced failure criteria, such as the Drucker-Prager criteria, are often suitable for analyzing the pressure-sensitive behavior of polymers, the von Mises criterion was selected to maintain methodological consistency with comparable FEA studies in prosthodontics.

Although ceramics are brittle, they are harder than composites and therefore provide greater wear resistance[34]. Hybrid ceramics, by contrast, have an elastic modulus similar to that of natural tooth tissue and combine the advantageous properties of both composite resins and dental ceramics[35]. With the development of composite-containing hybrid ceramics, partially fixed restorations aim to achieve not only superior aesthetics but also physical properties similar to those of natural tooth structures[36,37].

Ceramics exhibit fracture resistance ranging from 160 to 450 MPa, high modulus of elasticity, favorable long-term survival rates, and low wear potential. Irrespective of the fabrication technique, glass-ceramic inlay and onlay restorations are reliable treatment options with high survival rates[38].

A 2020 meta-analysis of 29 studies evaluated the success and survival of onlay restorations fabricated from ceramic, hybrid ceramic, and composite materials, reporting survival rates of 90%, 99%, and 98% for composites, hybrid ceramics, and lithium disilicate ceramic, respectively, over 24–180 months of follow-up[39].

A systematic review conducted by Morimoto *et al.*[40] determined that ceramic onlay restorations demonstrated superior clinical outcomes compared with composite onlay restorations. The reliability of zirconia for inlay restorations has been validated based on both clinical and laboratory findings[41]. The results obtained in this study with the zirconia-containing LithaCon 3y210 material further corroborate these findings.

Yamanel *et al.*[42] assessed the von Mises stresses across two composite and two ceramic inlay/onlay systems under a 200 N load and found that ceramic materials exhibited higher stress concentrations. Consistent with these findings, we observed higher von Mises stress values in ceramic inlays (833.04 MPa) than in composite-containing ceramic inlays (728.16 MPa) under a 300 N loading condition.

The ranking in terms of elastic modulus was zirconia > gold > leucite > composite in a study evaluating four different coronal restorative materials using 3D finite element stress analysis. The magnitudes of stresses observed in the underlying dentin tissue followed an inverse pattern, with the highest values obtained for the composite and the lowest for zirconia, indicating that stresses in the dentin decreased as the elastic modulus increased[43]. Parallel with this study, the highest stress value (1225.88 MPa) in the present work

was detected in the zirconia-containing material (LithaCon 3y210), whereas the lowest value (434.03 MPa) was found in the composite-containing material (VarseoSmile Crown Plus).

Yamanel *et al*.[42] reported that zirconia and lithium disilicate effectively absorb stress by transmitting less stress when placed over substructures with lower moduli of elasticity. These findings are consistent with those of the *in vitro* studies conducted by Waldecker *et al*.[44], which confirmed the durability of zirconia in complex clinical situations. These studies demonstrate that zirconia remains stable and functional even under high mechanical stress, making it an ideal option for long-term restorations[44].

Although 3D-printed composites show promise for use in temporary restorations, additional mechanical reinforcement is required to enhance their performance for permanent use. Our results agree with those of Alshamrani *et al*., who reported higher stress concentrations in the occlusal regions of these materials[45].

Owen and Hinto[46] stated that the number of elements and nodes used in the modeling process is a critical factor in determining the accuracy of analysis results, and that an increase in the element count brings the simulation results closer to reality. Therefore, the maximum possible number of elements was selected within the capacity of the software, considering the dimensions of the tooth model. Different numbers of elements and nodes were utilized for each model analysis.

From a clinical perspective, the results of this study suggest that the material selection should be tailored to the biomechanical status of the remaining tooth structure. Overlay designs fabricated from high-modulus materials (such as LithaCon 3Y-210) are advantageous for molars with compromised or thin cusps. These materials exhibit a "stress-shielding" effect by taking on the load and reducing the stress transmitted to the underlying dentin, thereby protecting weakened tooth structures. Conversely, for conservative preparations, in which a substantial tooth structure remains (such as inlays), low-modulus materials (such as VarseoSmile or Lava Ultimate) may be preferable because of their stress-absorbing damping capabilities, provided that the adhesive interface is meticulously executed. However, clinicians must be aware that although flexible materials reduce the internal restoration stress, they transfer more load to the tooth-restoration interface.

Finally, this study has several limitations. First, the dental tissues (enamel and dentin) were modeled as isotropic, linear, and homogeneous elastic materials, thus simplifying their complex nature. Natural tooth structures exhibit anisotropic behavior. Similarly, the periodontal ligament (PDL) was simulated as a linear elastic material and demonstrated nonlinear viscoelastic behavior *in vivo*. However, modeling these complex microstructural properties requires excessive computational resources and is often prone to convergence errors. Given that the primary objective of this study was to compare the relative mechanical behaviors of different restorative materials under identical conditions, these standard simplifications were maintained to ensure computational feasibility and did not compromise the qualitative validity of the comparative results. Second, the loading condition was static, and fatigue loading or thermal cycling was not simulated. Third, the resin cement layer was not modeled as a separate volume; instead, a perfect bonding interface was assumed. Consequently, the stress accumulation within the cement layer could not be evaluated. Fourth, oblique or lateral forces, which occur during mandibular excursions, typically generate higher tensile and shear stresses compared to vertical loading. If oblique forces were applied, stress concentrations would likely have shifted from the compressive zones on the pulpal floor to the cervical margins and restoration-tooth interface, potentially increasing the risk of debonding or fracture. However, the vertical loading protocol used in this study provides a valid baseline for comparing the relative stiffnesses and shock-absorbing potentials of the tested materials. Although FEA effectively identifies stress concentration areas that are prone to failure, it cannot directly predict the clinical longevity or long-term survival rates of restorations. The results should be interpreted as a comparative assessment of the initial biomechanical risks, rather than as a prediction of service life. In the present study, individual color scales were maintained for each component to clearly visualize the stress distribution patterns within materials with significantly different mechanical properties (e.g., enamel vs. luting cement). This approach avoids masking the stress gradients in lower-stiffness structures and is consistent with recent finite element studies[47,48]. Future studies should incorporate fatigue scenarios to further validate these findings.

## 5. Conclusions

Within the limitations of this FEA, it was concluded that the restoration design and material stiffness significantly influenced the stress distribution. Specifically, overlay designs fabricated from high-elastic-modulus 3D-printed zirconia (3Y-TZP) (such as LithaCon 3Y-210) provide the most favorable biomechanical environment by exhibiting a stress-shielding effect, thereby reducing stress transmission to the remaining tooth structure. This combination outperformed conservative inlay designs restored with low-modulus materials (such as VarseoSmile Crown Plus and Lava Ultimate), which transferred higher stress loads to the dentin. Consequently, overlay designs with 3D-printed zirconia ceramics are recommended for posterior teeth with extensive structural loss to reinforce the remaining cusps and minimize the risk of tooth fracture.

## Ethics statement

This study used de-identified CT-based models without direct human or animal involvement and was approved by the Non-Interventional Clinical Research Ethics Committee, Recep Tayyip Erdoğan University (decision no: 2025/383; meeting date: Sep 11, 2025; official letter date: Sep 17, 2025; ref no: E-40465587-050-1721). Document verification code: 228c79b5e001 (verification address available from the institution).

## Funding

This study has been supported by the Recep Tayyip Erdoğan University Development Foundation (grant ID 02025011017781).

We would like to thank the Scientific Research Projects Unit of Recep Tayyip Erdoğan University for supporting this study under project number TDH-2024-1836.

## Conflicts of interest

The authors declare no conflicts of interest.

## References


[1] Grivas E, Roudsari RV, Satterthwaite JD. Composite inlays: a systematic review. Eur J Prosthodont Restor Dent. 2014;22:117–24. PMID:25831713

[2] Edelhoff D, Ahlers MO. Occlusal onlays as a modern treatment concept for the reconstruction of severely worn dentition. J Prosthet Dent. 2018;120:677–84.

[3] Spitznagel FA, Scholz KJ, Strub JR, Vach K, Gierthmuehlen PC. Polymer-infiltrated ceramic CAD-CAM inlays and partial coverage restorations: 3-year results of a prospective clinical study over 5 years. Clin Oral Investig. 2018;22:1973–81. https://doi.org/10.1007/s00784-017-2293-x, PMID:29214376

[4] Rocca GT, Rizcalla N, Krejci I, Dietschi D. Evidence-based concepts and procedures for bonded inlays and onlays. Part II. Guidelines for cavity preparation and restoration fabrication. Int J Esthet Dent. 2015;10:392–413. PMID:26171443

[5] Burgess JO, Haveman JR, Butner RO. Resin-based composite systems. Dent Clin North Am. 2002;46:341–65.

[6] Trushkowsky RD, Burgess JO. Complex single-tooth restorations. Dent Clin North Am. 2002;46:341–65. https://doi.org/10.1016/S0011-8532(01)00002-7, PMID:12014037

[7] Veneziani M. Posterior indirect adhesive restorations: updated indications and the Morphology Driven Preparation Technique. Int J Esthet Dent. 2017;12:204–30. PMID:28653051

[8] El-Damanhoury HM, Haj-Ali R, Platt JA. Fracture resistance and marginal adaptation of ceramic occlusal veneers with different preparation designs: A systematic review. J Esthet Restor Dent. 2022;34:156–67.

[9] Revilla-León M, Sadeghpour M, Özcan M. An update on applications of 3D printing technologies used for processing polymers, metals, and ceramics in dentistry. J Prosthodont. 2020;29:205–13.

[10] Malament KA, Margvelashvili-Malament M, Natto ZS, Thompson V, Rekow D, Att W. 10.9-year survival of pressed acid etched monolithic e.max lithium disilicate glass-ceramic partial coverage restorations: performance and outcomes as a function of tooth position, age, sex, and the type of partial coverage restoration (inlay or onlay). J Prosthet Dent. 2021;126:523–32. https://doi.org/10.1016/j.prosdent.2020.07.015, PMID:33012530

[11] Fathy SM, Al-Zordk W, Grawish ME, Puckett AD. Flexural strength and translucency characterization of aesthetic monolithic CAD/CAM materials. J Esthet Restor Dent. 2021;33:913–21.

[12] Alamoush RA, Silikas N, Satterthwaite JD. The effect of resin-matrix ceramics on the stress distribution of endodontically treated teeth: A finite element analysis. J Prosthet Dent. 2021;126:409–16.

[13] Revilla-León W, Meyer MJ, Özcan M. Metal additive manufacturing technologies: literature review of current status and future perspectives in restorative dentistry. Int J Comput Dent. 2019;22:55–67. PMID:30848255

[14] Falcinelli C, Valente F, Vasta M, Traini T. Finite element analysis in implant dentistry: state of the art and future directions. Dent Mater. 2023;39:539–56. https://doi.org/10.1016/j.dental.2023.04.002, PMID:37080880

[15] Zheng Z, Sun J, Jiang L, Wu Y, He J, Ruan W, *et al.* Influence of margin design and restorative material on the stress distribution of endocrowns: a 3D finite element analysis. BMC Oral Health. 2022;22:30. https://doi.org/10.1186/s12903-022-02063-y, PMID:35120525

[16] Meng Q, Zhang Y, Chi D, Gong Q, Tong Z. Resistance fracture of minimally prepared endocrowns made by three types of restorative materials: a 3D finite element analysis. J Mater Sci Mater Med. 2021;32:137. https://doi.org/10.1007/s10856-021-06610-x, PMID:34716807

[17] Wendler M, Belli R, Petschelt A, Mevec D, Harrer W, Lube T, *et al.* Chairside CAD/CAM materials. Part 2: flexural strength testing. Dent Mater. 2017;33:99–109. https://doi.org/10.1016/j.dental.2016.10.008, PMID:27884403

[18] Tanaka IV, Tribst JPM, Silva-Concilio LR, Bottino MA. Effect of different ceramic materials on fatigue resistance and stress distribution in upper canines with palatal veneers. Eur J Dent. 2022;16:856–66. https://doi.org/10.1055/s-0041-1740225, PMID:35114726

[19] Lithoz Gmb H. Material overview–LithaCon 3Y 210 | 3Y 230: technical data. *2024;* and Callister WD, Rethwisch DG. Materials science and engineering: an introduction. 10th ed. Wiley; 2020.

[20] Prause E, Malgaj T, Kocjan A, Beuer F, Hey J, Jevnikar P, *et al.* Mechanical properties of 3D-printed and milled composite resins for definitive restorations: an in vitro comparison of initial strength and fatigue behavior. J Esthet Restor Dent. 2024;36:391–401. https://doi.org/10.1111/jerd.13132, PMID:37680013

[21] Van Dalen A, Feilzer AJ, Kleverlaan CJ. In vitro exploration and finite element analysis of failure mechanisms of resin-bonded fixed partial dentures. J Prosthodont. 2008;17:555–61. https://doi.org/10.1111/j.1532-849X.2008.00349.x, PMID:18761569

[22] Giannini M, Soares CJ, de Carvalho RM. Ultimate tensile strength of tooth structures. Dent Mater. 2004;20:322–9. https://doi.org/10.1016/S0109-5641(03)00110-6, PMID:15019445

[23] Corsentino G, Pedullà E, Castelli L, Liguori M, Spicciarelli V, Martignoni M, *et al.* Influence of access cavity preparation and remaining tooth substance on fracture strength of endodontically treated teeth. J Endod. 2018;44:1416–21. https://doi.org/10.1016/j.joen.2018.05.012, PMID:30049468

[24] Hopp C, Land MF. Considerations for ceramic inlays in posterior teeth: a review. Clin Cosmet Investig Dent. 2013;5:21–32. https://doi.org/10.2147/CCIDE.S42016, PMID:23750101

[25] Ho MH, Lee S, Chen HH, Lee MC. Three-dimensional finite element analysis of the effects of posts on stress distribution in dentin. J Prosthet Dent. 1994;72:367–72. https://doi.org/10.1016/0022-3913(94)90555-X, PMID:7990041

[26] Hidaka O, Iwasaki M, Saito M, Morimoto T. Influence of clenching intensity on bite force balance, occlusal contact area, and average bite pressure. J Dent Res. 1999;78:1336–44. https://doi.org/10.1177/00220345990780070801, PMID:10403461

[27] Gibbs CH, Mahan PE, Lundeen HC, Brehnan K, Walsh EK, Holbrook WB. Occlusal forces during chewing and swallowing as measured by sound transmission. J Prosthet Dent. 1981;46:443–9. https://doi.org/10.1016/0022-3913(81)90455-8, PMID:6946215

[28] Yoon HG, Oh HK, Lee DY, Shin JH. 3-D finite element analysis of the effects of post location and loading location on stress distribution in root canals of the mandibular 1st molar. J Appl Oral Sci. 2018;26:e20160406. https://doi.org/10.1590/1678-7757-2016-0406, PMID:29451648

[29] Dartora G, Rocha Pereira GK, Varella de Carvalho R, Zucuni CP, Valandro LF, Cesar PF, *et al.* Comparison of endocrowns made of lithium disilicate glass-ceramic or polymer-infiltrated ceramic networks and direct composite resin restorations: fatigue performance and stress distribution. J Mech Behav Biomed Mater. 2019;100:103401. https://doi.org/10.1016/j.jmbbm.2019.103401, PMID:31445400

[30] Tribst JPM, Dal Piva AMO, Madruga CFL, Borges ALS, Bottino MA, Kleverlaan CJ. Biomechanical evaluation of different filling techniques for class II restorations. Materials (Basel). 2020;13:3852.

[31] Zhang Y, Lawn BR. Novel zirconia materials in dentistry. J Dent Res. 2018;97:140–7. https://doi.org/10.1177/0022034517737483, PMID:29035694

[32] Yap AU, Hussein LS, Yang B. Influence of C-factor and light-curing mode on shrinkage forces and fracture toughness of bulk-fill composites. Oper Dent. 2021;46:216–26.

[33] Giannessi E, Stornelli MR, Sergi PN. Strain stiffening of peripheral nerves subjected to longitudinal extensions in vitro. Med Eng Phys. 2020;76:1–12. https://doi.org/10.1016/j.medengphy.2019.10.012

[34] Fron-Chabouis H, Faugeron VS, Attal JP. Clinical efficacy of composite versus ceramic inlays and onlays: A systematic review. Dent Mater. 2013;29:1209–18. https://doi.org/10.1016/j.dental.2013.09.009, PMID:24119328

[35] Amesti-Garaizabal A, Agustín-Panadero R, Verdejo-Solá B, Fons-Font A, Fernández-Estevan L, Montiel-Company JM, *et al.* Fracture resistance of partial indirect restorations made with CAD/CAM technology. A systematic review and meta-analysis. J Clin Med. 2019;8:1932. https://doi.org/10.3390/jcm8111932, PMID:31717610

[36] Zafar MS, Amin F, Fareed MA, Ghabbani H, Riaz S, Khurshid Z, *et al.* Biomimetic aspects of restorative dentistry biomaterials. Biomimetics (Basel). 2020;5:34. https://doi.org/10.3390/biomimetics5030034, PMID:32679703

[37] Bijelic-Donova J, Keulemans F. Direct bilayered biomimetic composite restoration: the effect of a cusp-supporting short fiber-reinforced base design on the chewing fracture resistance and failure mode of molars with or without endodontic treatment. J Mech Behav Biomed Mater. 2020;103:103554. https://doi.org/10.1016/j.jmbbm.2019.103554, PMID:32090948

[38] Rebello de Sampaio FBW, Özcan M, Gimenez TC, Moreira MSCA, Tedesco TK, Morimoto S. Effects of manufacturing methods on the survival rate of ceramic and indirect composite restorations: A systematic review and meta-analysis. J Esthet Restor Dent. 2019;31:561–71. https://doi.org/10.1111/jerd.12555, PMID:31840412

[39] Bustamante-Hernández N, Montiel-Company JM, Bellot-Arcís C, Mañes-Ferrer JF, Solá-Ruíz MF, Agustín-Panadero R, *et al.* Clinical behavior of ceramic, hybrid, and composite onlays: systematic review. Int J Environ Res Public Health. 2020;17:7582. https://doi.org/10.3390/ijerph17207582, PMID:33086485

[40] Morimoto S, Rebello de Sampaio FBW, Braga MM, Sesma N, Özcan M. Survival rate of resin and ceramic inlays, onlays, and overlays: A systematic review and meta-analysis. J Dent Res. 2016;95:985–94. https://doi.org/10.1177/0022034516652848, PMID:27287305

[41] Bömicke W, Rathmann F, Pilz M, Bermejo JL, Waldecker M, Rammelsberg P, *et al.* Clinical performance of monolithic zirconia resin-bonded fixed dental prostheses: a randomized controlled trial. J Prosthodont. 2020;29:1–9.

[42] Yamanel K, Caglar A, Gulsahi K, Ozden UA. Effects of different ceramic and composite materials on stress distribution in inlay and onlay cavities: 3-D finite element analysis. Dent Mater J. 2009;28:661–70. https://doi.org/10.4012/dmj.28.661, PMID:20019416

[43] Dejak B, Młotkowski A, Langot C. Three-dimensional finite element analysis of molars with thin-walled prosthetic crowns made of various materials. Dent Mater. 2012;28:433–41. https://doi.org/10.1016/j.dental.2011.11.019, PMID:22209573

[44] Waldecker M, Rues S, Rammelsberg P, Bömicke W. Validation of in-vitro tests of zirconia-ceramic inlay-retained fixed partial dentures: A finite element analysis. Dent Mater. 2019;35:e53–62. https://doi.org/10.1016/j.dental.2019.01.017, PMID:30686709

[45] Alshamrani A, Fahimipour A, Alsarani M, Ellakwa A. Flexural properties and finite element analysis of novel three-dimensional printed ceramics fabricated via lithography-based ceramic manufacturing. Aust Dent J. 2024;69:123–32.

[46] Owen JT, Hinton E. A simple guide to finite elements. Swansea: Pineridge Press, 1983:1-12.

[47] Xu J, Ma J, Tan Z, Zhang Q, Hu J, Li J. A 3D-FEA study on the impact of different preparation forms and materials on posterior occlusal veneers. J Mech Behav Biomed Mater. 2024;152:106462. https://doi.org/10.1016/j.jmbbm.2024.106462, PMID:38346366

[48] Chirca O, Biclesanu C, Florescu A, Stoia DI, Pangica AM, Burcea A, *et al.* Adhesive-ceramic interface behavior in dental restorations. FEM study and SEM investigation. Materials (Basel). 2021;14:5048. https://doi.org/10.3390/ma14175048, PMID:34501143